Scholar Publishing Group
International Journal of Health and Pharmaceutical Medicine
https://doi.org/10.38007/IJHPM.2022.030404
ISSN 2789-8393 Vol. 3, Issue 4: 41-53

Image and Diagnosis Analysis of Multi-Slice Spiral CT and Chest X-Ray of Neonatal Pneumonia

Liulin Wang*

Guangzhou College of SCUT, Guangzhou, China

**corresponding author*

Keywords: Neonatal Pneumonia, Multi-Slice Spiral CT, Spiral Interpolation, Mycoplasma Pneumonia

Abstract: Among all neonatal diseases, neonatal pneumonia is one of the common diseases. Multi-slice spiral CT and chest X-ray imaging images are used to diagnose and study neonatal pneumonia in hospitals and treat neonates in China. Pneumonia is of great significance. This article retrospectively analyzes the CT and chest X-ray images of neonatal pneumonia, and divides the cases into two groups according to their invasiveness: pre-invasive and micro-invasive group, invasive group, and the size of the air-containing cavity Analyze the multiple occurrence and distribution position; observe the air-containing cavity structure morphology under the microscope. All patients were scanned by the chest multi-slice spiral CT scanner, and the 1m or 0.625m thin-slice images were sent to the post-processing workstation for statistics and analysis of relevant data. This article discusses the entire calculation process from projection data preprocessing to spiral interpolation to image reconstruction of neonatal pneumonia. The effects of the two interpolation modes on the reconstruction results are compared. A practical multi-layer spiral cone beam algorithm is given. An important aspect of the performance of neonatal pneumonia image performance and its generation mechanism are analyzed. As an equipment manufacturer, it provides a basis for the improvement and correction of machine performance. This article analyzes the real-time fluorescence quantitative PCR value of neonatal Mycoplasma pneumoniae and its gender, Relevance of age, heat history, heat type, shortness of breath, wheezing, atelectasis, pleural effusion and ventilator ventilation treatment, and the study subjects were divided into two groups according to whether they were treated with macrolide antibiotics. After heterogeneity, the relationship between the severity of the disease and the pathogen load and inflammation in the two groups was studied. The results of the study show that RSV is the most common viral pathogen of neonatal pneumonia, and the risk of repeated wheezing in children with RSV and Klebsiella pneumoniae is continuously increasing within 3 years of age, but the occurrence between the two There was no statistical difference in risk.

1. Introduction

Newborns are at high risk of infection due to immature lung tissue development, low immune

defense function, and imperfect skin and mucosal barrier. The community environment is complex, and there may be a variety of infectious pathogenic microorganisms, such as viruses, bacteria, etc., which can easily invade newborns through contact, droplets and other means. The respiratory tract is the most vulnerable part, and pneumonia can spread downward from the upper respiratory tract. Pneumonia is still the world's leading cause of death among children under five, and the neonatal period is the stage with the highest risk of death from pneumonia.

Respiratory tract infections are closely related to wheezing. At present, a large number of studies have reported that viral infections, especially respiratory syncytial virus, can easily induce or aggravate wheezing attacks in children. In recent years, with the continuous in-depth research on wheezing diseases, there are gradually reports in the literature that bacteria and wheezing are also closely related. Mahnken et al. conducted a meta-analysis of 31 birth cohort studies and found that preterm infants and low birth weight infants increased the risk of preschool wheezing. In full-term newborns, the relationship between respiratory viruses and bacteria is not clear. Therefore, this study aims to explore the impact of co-detection of viruses and bacteria on the severity of pneumonia in full-term neonates, and whether the co-detection will increase during follow-up the risk of recurrent wheezing, eczema, and allergic rhinitis in the later period [1]. Rahmati observed that RSV was positively correlated with Haemophilus influenzae in the upper respiratory etiology test of children under 2 years of age. The results show that RSV in neonatal pneumonia is more likely to be detected with Escherichia coli, Klebsiella pneumoniae, Staphylococcus aureus, and Enterobacter cloacae, which is inconsistent with the above research results, which may be due to differences in region, race and age[2]. Joob analyzed the distribution of pathogens in neonatal pneumonia and found that the most common Gram-negative bacteria were Escherichia coli, Klebsiella pneumoniae, Haemophilus influenzae, and the most common Gram-positive bacteria were Staphylococcus aureus Bacteria, consistent with the results of this study [3].

In recent years, my country has successively discovered that bacterial colonization or infection in the respiratory tract may cause or aggravate the onset of wheezing, resulting in repeated wheezing in the later period, and eventually developing asthma. Gentile reported that there is a significant difference in the bronchial bacterial microbiota between children with allergic asthma and healthy controls. After colonization or infection of the respiratory tract, Gram-negative bacteria release a large amount of endotoxin, aggravate neutrophil inflammation, Th1/Th2 immune response imbalance, cause airway hyperresponsiveness and airway inflammation, and ultimately lead to the occurrence or aggravation of wheezing [4]. Lin conducted research on asymptomatic newborns and found that one or more of the bacteria such as Streptococcus pneumoniae, Haemophilus influenzae, and Moraxella catarrhalis colonized the respiratory tract, which increased the children's first wheezing, persistent wheezing, and acute exacerbations of wheezing[5].

This paper effectively improves the quality of CT image reconstruction by solving the problems of uneven illumination of projection images and misalignment of background images that are common in the process of CT imaging. The filter method is combined with the numerical correction of the projection image based on the standard sample. A method for correcting the effect of beam hardening in CT imaging. The findings of this article not only help to eliminate CT image artifacts, but also provide a basis for the development of quantitative CT characterization techniques.

2. Newborn Pneumonia Multi-Slice Spiral CT and Chest X-Ray Imaging Image and Diagnosis Research

2.1. Comparative Study of CT Image Performance and Pathology of Neonatal Lungs

(1) Image analysis

It should be noted that when judging whether the air-containing cavity structure exists, it should

be observed on the multi-plane and multi-angle thin-layer image to exclude the bronchus passing through; the blood vessel changes include the thickening of the blood vessel in the lesion and the change in shape (distortion) , Stiffness, focus in the lesion), observe on the thin-slice cross-sectional image and MPR image, the order is from the right hilum to the periphery of the lung, and the radial distribution, and the tapered ones are regarded as normal blood vessels, if they lose their natural Morphology, tapering characteristics, even the distal end is thicker than its proximal end or thicker than the surrounding blood vessels at the same level, it can be regarded as thickening of the blood vessel (thickening in the lesion or before entering the lesion); if the blood vessel goes away from the normal path, then It is regarded as twisted; if the small blood vessels around the lesion are also seen to deviate from the normal direction and the lesion is concentrated, it is regarded as a vascular cluster.

(2) Nodule segmentation and image texture feature parameter extraction

The 104 pGNs are segmented. The segmentation method is semi-automatic segmentation, that is, first import the original DICOM of each case into a computer equipped with the image texture feature analysis software developed by United Imaging, and the computer automatically recognizes the pneumonia interface of pGNs and performs automatic segmentation. Among them, 10 pGNs failed to segment. Next, an experienced diagnostic imaging physician checked the automatic segmentation results of 94 pGNs and manually adjusted them. Another physician was responsible for retesting the semi-automatic segmentation results. The final goal was to make the segmentation line Good distribution along the pneumonia interface of the nodule [6-7].

2.2. The Main Impact of CT Image Reconstruction

In image reconstruction, the factors that affect reconstruction are summarized as follows: Various errors in data acquisition: data acquisition method and acquisition amount, and reconstruction algorithm used.

(1) Various errors in data collection:

Reliable and efficient data is the foundation of any reconstruction algorithm. In CT, due to the limitations of various physical conditions, various errors will occur in the actual measurement process of obtaining projection data, which are mainly manifested in the following aspects.

1) Due to the statistical characteristics of X-ray photon generation, photon-matter interaction and photon detection, errors will inevitably occur in the measurement data. It can be considered that the number of photons in the detector obeys the Poisson distribution, and when the average value is high, it is approximately Gaussian distribution [8-9]. Since the measurement error is also a random variable, it can be treated as a Gaussian distribution with zero mean. Some reconstruction algorithms take advantage of these characteristics.

2) In CT, X-rays commonly used are composed of photons of different energies, called polychromatic X-rays; for low-energy photons, the attenuation is usually relatively large at a certain point, so when X-rays pass through an object, the spectral energy distribution is changing. This phenomenon is called beam hardening [10-11]. In TCT, the reconstruction attenuation factor needs to reduce the beam in the same way at a specific point, which can only be achieved by using monochromatic X-rays, and usually monochromatic projection data is obtained by correcting the polychromatic projection data obtained from it. experiment. Bundling reinforcement corrections can also cause data errors.

3) The so-called partial volume effect caused by the focal point of the light source and the size of the detector, the efficiency of the detector and the stability of the device are all sources of error in data collection [12-13]. Some errors can be corrected correctly by hardware, while other errors need to be corrected by algorithms. Due to the inevitable errors in the measurement data, when

discussing reconstruction issues, we need to involve algorithm stability and reconstruction error analysis.

(2) Reconstruction of incomplete projection data

In many cases, due to the limitations of objective conditions, the problem of incomplete data reconstruction is often encountered. The debate on reconstruction of such issues is of great significance not only in theory but also in practical applications [14-15]. This type of problem can be attributed to the following situations:

1) Angle limitation problem

This type of incomplete projection data is caused by the inability to collect projection data at a specific angle, which leads to a defect in the coverage of the projection angle. In non-destructive industrial testing, limited collection time or obstacles around the detection area will result in such incomplete projection data [16-17]. The main methods to solve this kind of incomplete data problem are: compression recovery method, ART method and various iterative bypass methods. However, this method often lacks theoretical quantitative analysis for the serious defects of this problem. Therefore, when the lack of data is greater, the reliability of the reconstruction results is questionable.

2) External issues

This type of incomplete projection data is caused by the inability to collect all projection data passing through a specific part of the detection area. This situation mainly occurs when there is an "opaque" substance in the detected radiation of the test object [18-19]. It can be derived from the Cormack inversion formula and uniquely determines the solution to the external problem. But this is also a problem of bad position. Appropriate standardized methods must be used. In this way, the image obtained by the inversion usually appears blurry at the edge tangent to the projection direction where the data is missing.

3) Internal issues

This type of incomplete projection data is created because the beam coverage may not include the entire object to be detected. This type of incomplete display data can occur when the detected object is too large or you only want to locate a local area ofinterest. Internal problems are also called partial image restoration problems [20-21]. In practical applications, the above three types of combinations are often encountered, and the reconstruction problem is currently more complicated. For the reconstruction of incomplete projection data, an optimized iterative reconstruction algorithm based on various reconstruction criteria is currently a relatively effective algorithm. The biggest advantage of this algorithm is that by adding various known prior knowledge to the iteration process for extrapolation, the estimated value of the missing projection data is obtained, so that the iteration result gradually approaches the original image.

2.3. Study on Pneumonia Caused by Virus and Bacteria Co-Infection in the Respiratory Tract of Newborns

Mycoplasma pneumoniae pneumonia is an acute respiratory infectious disease caused by droplet transmission. The real-time fluorescent quantitative PCR value of Mycoplasma pneumoniae in children is related to the heat type of the children. The clinical and imaging manifestations of Mycoplasma pneumoniae pneumonia are related to its pathogen load and inflammation [22-23]. Not only need anti-infective treatment with macrolide antibiotics, but also glucocorticoid anti-inflammatory treatment for severely ill children.

After Mycoplasma pneumoniae invades the human respiratory tract, it adheres to the epithelial cells of the human respiratory mucosa in a special way to resist the clearing of cilia and the phagocytosis of phagocytes. Mycoplasma pneumoniae itself releases some toxic metabolites,

causing the destruction of respiratory epithelial cells, thus causing the corresponding pathological changes, which is its main pathogenesis. In the early stage of infection, the human body's non-specific immune mechanism will cause the corresponding cells to secrete inhibitors and complement, accompanied by phagocytosis of phagocytes. After two weeks, the concentration of complement begins to decrease, causing the surface of neutrophils to contact Mycoplasma pneumoniae and infection the human body begins to produce IgM after 7-15 days, and its concentration reaches a peak in 3-4 weeks and lasts for several months.

(1) Reduce the removal of bacteria

The epithelial layer of the respiratory tract is the first line of defense against bacterial infections, and the destruction of this barrier by viruses leads to reduced bacterial clearance. The destruction of mucociliary function by IAV, RSV and ADV reduces the clearance of Streptococcus pneumoniae and Haemophilus influenzae. RSV inhibits the expression of antimicrobial peptides in the nasopharynx, thereby reducing the clearance of Streptococcus pneumoniae. Respiratory virus infection can inhibit the immune protective response of innate immune cells [24-25]. Such innate immune cells mainly include macrophages, neutrophils, natural killer cells and so on. IAV has been proven to induce the death of alveolar macrophages and interfere with early pneumococcal clearance. The synergistic stimulation of IAV and Streptococcus pneumoniae causes high expression of IFN-γ, inhibits the recruitment of macrophages in mouse lungs, reduces the bactericidal activity of macrophages, and prevents the body from effectively removing bacteria. In influenza virus infection, virus-induced glucocorticoids and IFN-I can inhibit the production of cytokines and chemokines, down-regulate the recruitment of neutrophils, and at the same time inhibit the secretion of TNF-α by natural killer cells to make macrophages the ability to swallow bacteria is inhibited.

(2) Increase the adhesion of bacteria

Virus infection of airway epithelial cells has been found to increase the adhesion of bacteria through certain mechanisms, although the effect is different on different viruses, strains, and experimental models. Free RSV virus particles can directly bind Streptococcus pneumoniae and Haemophilus influenzae, so that the bacteria can approach the epithelial monolayer cells and increase the adhesion to the host cell receptor. RSV-infected host cell membranes have adherent G glycoproteins, which can act as receptors for bacteria. Respiratory viruses can also up-regulate the expression of host cell surface proteins, and bacteria can combine with them to facilitate the growth of bacteria. Neuraminidase of influenza virus activates transforming growth factor β to up-regulate bacterial host adhesion factors, such as fibronectin, integrin, etc., and increase the load of bacteria in the lungs. In addition, cell receptors that adhere to bacteria have also been exposed to viral neuraminic acid activity. Virus-induced cell death can lead to exposure of the epithelial basement membrane and increase bacterial adhesion.

(3) Suppress immunity during recovery

During the recovery process of primary viral infection, the host's susceptibility to secondary bacterial infection may still be high. With the clearance of the virus, the homeostasis of the lung environment is restored, and inflammation-mediated healing of the lung injury begins. In this process, to ensure adequate healing, the inflammatory response is suppressed. However, these mechanisms may also promote the colonization of lower respiratory tract bacteria and secondary bacterial infections. The recovery process after influenza A virus infection is dominated by the excessive release of interleukin (IL) 10, which inhibits the identification and removal of bacteria in the lungs, which may lead to secondary bacterial infections in the later stage when the viral disease is close to recovery.

(4) Bacteria's regulation of virus infection

The Streptococcus pneumoniae conjugate vaccine not only reduces the incidence of pneumonia

caused by pneumococcus, but also reduces respiratory virus-associated pneumonia by approximately 33%.

The reduction of Streptococcus pneumoniae may also reduce children's susceptibility to viral infections. Similarly, the seroconversion rate of human metapneumovirus in children under 2 years of age is related to the nasopharyngeal carrying of Streptococcus pneumoniae. The in vitro test of pre-culture of human bronchial epithelial cells and Streptococcus pneumoniae also demonstrated the susceptibility of the cells to human metapneumovirus.

Bacteria may also promote virus replication or release in airway cells. Streptococcus pneumoniae after IAV infection has been found to cause an increase in virus titer. According to mathematical model evaluation, this increase may be related to the bacteria's increased production of virus particles and the promotion of the release of infected cells. Influenza virus needs to use protease to cleave and activate the glycoprotein of hemagglutinin before it becomes infectious. The bacterial protease secreted by Staphylococcus aureus can promote the activation of influenza virus hemagglutinin protein, increase the amount of virus replication in the lungs, and enhance its infectivity and pathogenicity.

(5) Related mechanisms to increase disease severity

Both influenza virus and Streptococcus pneumoniae can produce cytokines through molecular pattern recognition receptors such as Toll-like receptors (TLR), causing signal cascades and inflammation. Streptococcus pneumoniae can bind to TLR2 and TLR4 on the cell surface; influenza virus can bind to TLR7, TLR8 and TLR3. The signal transduction pathway of TLR2 is similar to that of TLR7 and TLR8. TLR4 and TLR3 have the same signal transduction pathway, which can cause pro-inflammatory cytokines such as IL-1, IL-6, IL-8, IL-10, and TNF. The generation of chemical factors. In addition, RSV can be recognized by the intracellular pattern recognition receptor NOD2, which can simultaneously recognize peptidoglycan in the cell wall of Streptococcus pneumoniae, leading to an inflammatory response. There is a potential overlap between the signaling pathways triggered by these two pathogens, which can cause co-stimulation of inflammation in mixed infections. Theoretically, an excessive inflammatory response can lead to the release of a large number of neutrophils and cytokine storms, thereby aggravating lung damage and significantly increasing the incidence.

3. Newborn Pneumonia Multi-Slice Spiral CT and Chest X-Ray Imaging Images and Diagnostic Experimental Research

3.1. Data and Collection

Collect data of newborn children who were hospitalized in the first respiratory ward and second respiratory ward of our hospital due to Mycoplasma pneumonia during 2018-2019. Inclusion criteria: respiratory symptoms or pulmonary signs throughout the course of the disease; MPPCR positive sputum in newborn children. Exclusion criteria: combined with chronic diseases such as tuberculosis and asthma; combined with airway dysplasia or other serious complications of the system. Finally, we included the data of 570 newborn children, of which 312 were male newborns, 258 were female newborns, 160 were newborn children under 3 years old, and 184 were newborn children aged 3-6 years. There are 155 cases of newborn children aged 6-9 years old, and 71 cases of newborn children older than 9 years old.

3.2. Imaging Analysis

Observe lung light transmittance, "ground glass" shadows, fine mesh shadows, granular shadows, thickening of the lobules, localized translucent shadows, irregular mediastinal edges, nodules, air

sac shadows, fibrosis and other lung manifestations, and count the number of nodules and airbags at the same time.

After 2 pediatric diagnostic imaging physicians with intermediate professional titles and above coordinated to read the pictures, the chest CT manifestations of 140 children were analyzed, and if there were differences, a consensus diagnosis conclusion was reached through consultation. 3.3 Image analysis

Send the image to the Agfa PACS system and the Philp intelispace portal workstation for observation, reconstruction and measurement.

(1) Definition of pure ground glass nodules

On the high-resolution CT window, the local lung tissue showed a fuzzy and mildly increased density shadow, but it did not affect the display of the bronchial vascular bundle, and it was completely invisible on the soft tissue window.

(2) Reconstruction method

Multi-plane reconstruction: Multi-angle reconstruction of the sagittal plane, coronal plane and oblique plane to facilitate the display of the morphological characteristics of the lesion; the minimum intensity projection level maximum intensity projection helps to display the blood vessels and bronchus; at the same time, the window width and window position can be fine-tuned to Achieve better image display effect. Two experienced doctors with experience in imaging diagnosis of chest diseases evaluate the post-processed images, and do not know the clinical data of the subject in advance, and analyze the size of the lesion and the average CT value respectively. The size of pGN adopts the largest long diameter of the largest cross-section of the nodule, repeats the measurement three times, and takes the average value; the average CT value is measured by dividing three regions of interest with an area of approximately 10m2 on the three largest planes of the pGN, taking three The average number of CT values for each region of interest.

CT features of pGN include edge (lobular sign, burr sign), morphology (round or quasi-circular, irregular), pneumonia interface (clearly smoothed, clear rough, fuzzy), internal structure (including air gap, air bronchus sign), adjacent structures (pleural depression sign, blood vessel changes) for analysis. Because the lung algorithm reconstruction will have a sharpening effect on the edge of the lesion, it is conducive to the display of the edge and shape of the lesion, but it will increase the measurement error of the CT value. Therefore, the measurement of the size of the lesion and the observation of signs are carried out in the reconstructed image of the lung algorithm. The CT value measurement is performed in the reconstructed image with the standard algorithm.

4. Newborn Pneumonia Multi-Slice Spiral CT and Chest X-Ray Imaging Images and Diagnostic Experimental Research Analysis

4.1. Correlation Study of Clinical Manifestations and Imaging Manifestations of Mycoplasma Pneumonia in Newborn Children

The subjects of this trial were 483 newborn children, of which group A was 328 children who were treated with macrolide antibiotics and then had fever after admission, and group B was for natural fever who were not treated with macrolide antibiotics. There were 185 children who retreated and did not have fever during the course of the disease. In order to determine the comparability of the clinical and imaging manifestations of the two groups of children, the experimental results are shown in Table 1 and Figure 1.

Table 1. Clinical and imaging manifestations of the two groups

	Group A	Group B
Hot journey (days)	10.74±3.57	5.38±4.25
High fever ratio	37.57%	12.47%
Shortness of breath	13.46%	9.43%
Breathing rate	13.76%	7.28%
Atelectasis ratio	26.48%	11.37%
Pleural effusion ratio	38.27%	10.37%

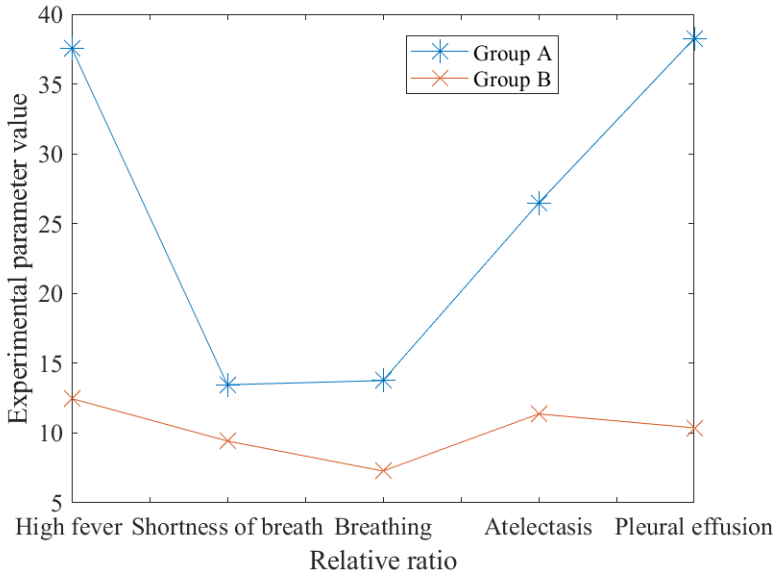

Figure 1. Clinical and imaging manifestations of the two groups

The study showed that the heat duration of group A and group B was 10.74±3.57d and 5.38±4.25d, respectively. The high fever rate was 37.57% in group A, 12.47% in group B, shortness of breath rate in group A was 13.46%, and group B was 9.43%. Wheezing The ratio of group A was 13.76%, group B was 7.28%, the atelectasis ratio was 26.48% in group A, 11.37% in group B, pleural effusion was 38.27% in group A, and group B was 10.37%. According to the observation of clinical manifestations and imaging results, the symptoms of group A are heavier than those of group B.

4.2. The Relationship between Lung CT Findings and Clinical Grade

Among 33 children with PLCH, pulmonary interstitial lesions were distributed in the clinical grades of grades Ⅰ to Ⅳ, with more distributions in grades Ⅲ and Ⅳ. Nodules and/or air sacs were distributed in grades Ⅱ to Ⅳ. There were only 2 cases with clinical grading, 1 case each with grade III and grade IV. There was no significant difference between the severity of lung CT findings and the clinical grade (P>0.05). As shown in Table 2 and Figure 2.

Table 2. CT findings and clinical scores of lungs (n, %)

	Level I (n=1)	Level II (n=7)	Grade Ⅲ (n=11)	Grade IV (n=14)	P value
Interstitial lung disease	2	6	12	16	
Airbag shadow	0	5	9	6	0.735
Pulmonary Fibrosis	1	1	0	2	

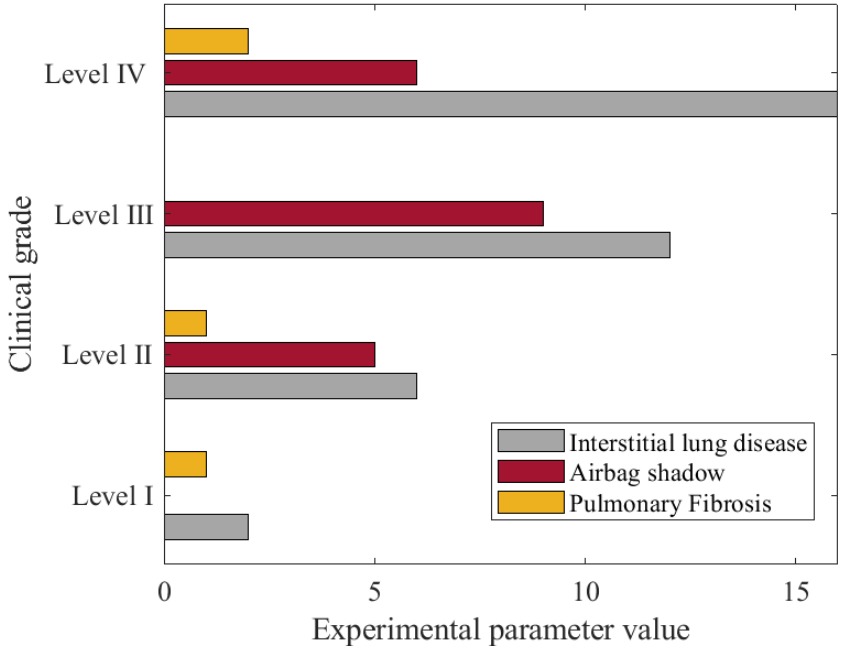

Figure 2. CT findings and clinical scores of lungs (n, %)

11 cases of children in this group were clinically treated (4 cases showed only pulmonary interstitial lesions, 4 cases showed pulmonary interstitial lesions with air sacs; 3 cases of nodules and air sacs, including 1 case with pulmonary fibrosis) Review the chest CT. 4 cases showed only pulmonary interstitial lesions, 2 cases of pulmonary interstitial lesions with air sac shadow, and 2 cases of nodules and air sac shadows were basically absorbed. One case showed decreased lung light transmittance and scattered air sacs before treatment. After 14 months of clinical treatment, the air sacs were slightly reduced and there were slight ground glass changes. An exception hospital had been misdiagnosed as polycystic lung. Before treatment, CT showed that the lungs were diffuse and air saccular with honeycomb and extensive fibrosis. After 4 months of treatment, the air sac was reduced, but there were fibers such as thick reticular shadows and striped shadows. The chemical manifestations persisted and were later lost to follow-up due to giving up treatment. One patient with extensive fine mesh shadows and scattered air sac shadows had persistent abnormalities in the lungs during short-term follow-up.

4.3. Survival Analysis 0f Risk Factors for Repeated Wheezing Within 3 Years of Age

Taking into account the inconsistent follow-up time of the included children, survival analysis was used to further analyze and conclude that the detection of RSV, Staphylococcus aureus and Klebsiella pneumoniae in neonatal pneumonia is a risk factor for recurrent wheezing within 3 years of age. In the RSV and Staphylococcus aureus co-detection group, the probability of recurrent wheezing within 3 years of age was 4.22 times that of the RSV group alone (HR, 4.22; 95% CI, 2.02-8.83; P<0.001). The risk ratio of recurrent wheezing in the RSV and Klebsiella pneumoniae co-detection group was 3.15 (95% CI, 1.51-6.57; P=0.002). As shown in Figure 3.

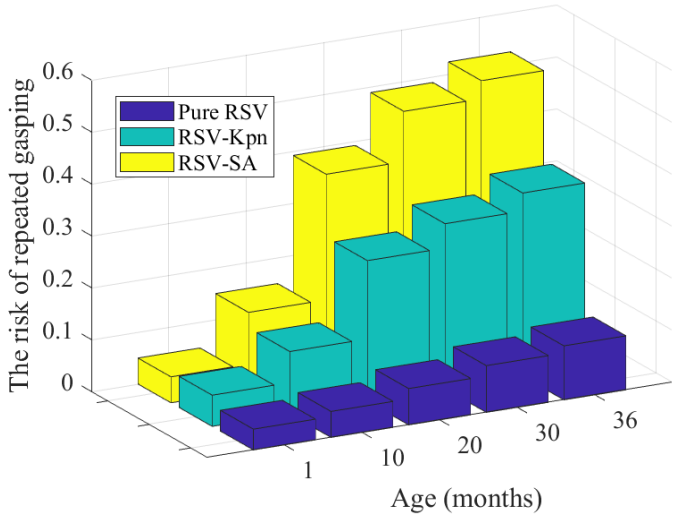

Figure 3. Comparison of the cumulative risk of recurrent wheezing in the simple RSV-positive group of newborns with RSV-Klebsiella pneumoniae and RSV-Staphylococcus aureus co-detection group

In this study, RSV is the most common viral pathogen of neonatal pneumonia, which is consistent with the results of other studies. The positive rate of RSV detection is about 10%, which is low. In the Kaplan-Meier analysis, the risk of repeated wheezing in children with RSV and Staphylococcus aureus and RSV and Klebsiella pneumoniae is continuously increasing within 3 years of age. But there was no statistical difference in the risk of occurrence between the two.

4.4. Actual Correction Result of CT Projection Image

For this CT experimental data, the specific value range of the fitting area D is 545<i<1264,1303<j<1840, and the fitting order n is 3. The correction models established for different projection images are different. Figure 4 shows the gray-scale curve of artificial sandstone in the projection image after monochromatic multi-spectral projection image.

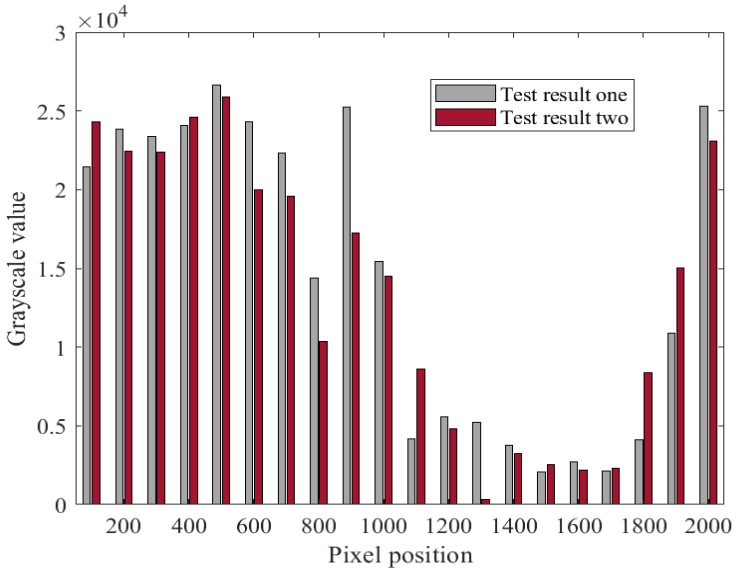

Figure 4. Gray value at the horizontal line

This paper establishes a CT image correction model for neonatal pneumonia. Using this model, the monochromatization of the X-ray projection data of CT images of neonatal pneumonia is realized to a certain extent. This method provides a new idea for correction of harness hardening effects and provides a basis for the development of quantitative CT characterization technology.

5. Conclusion

Based on the application prospects of X-ray CT for quantitative characterization of materials, this paper studies the problems of uneven illumination and background inconsistencies in the projection image during the CT experiment. Based on the problem of the beam hardening effect in the CT characterization technology, the gray data of the projection image A series of explorations were carried out on the harness hardening correction method. However, due to time constraints, some work has not yet been completed, and the study can be continued in the follow-up study. Mainly include: This article adopts dual-energy CT experiment, in order to realize the quantitative characterization research of industrial CT combined with DCM model.

Acute respiratory infections are the most common cause of early childhood illness and death worldwide. Recent studies have found that virus/bacterial co-infection is common, and it is important to understand the mechanism and clinical significance of co-infection. The application of the research results of these mechanisms to clinical work still needs to be further explored in order to provide patients with the best possible care, rational use of antibacterial drugs, and improve the understanding of chronic allergic and inflammatory diseases such as asthma.

The pathogenesis of RMPP in children is mainly related to factors such as MP resistance, immune dysfunction, mixed infection and hypercoagulable state. Clinically, if children who are not treated with macrolide antibiotics for 5 to 7 days, RMPP should be considered. Some children can be added with glucocorticoids for anti-inflammatory, and intravenous gamma globulin can be given supportive treatment if necessary. If the respiratory secretions are significantly increased and viscous, bronchoscopy lavage can be used to improve lung ventilation and ventilation function, shorten the course of disease, and reduce the occurrence of complications.

References

[1] Mahnken A H , Wildberger J E , Sinha A M , et al. Value of 3D-volume rendering in the assessment of coronary arteries with retrospectively ECG-gated multislice spiral CT.. Acta Radiologica, 2015, 44(3):302-309.https://doi.org/10.1080/j.1600-0455.2003.00057.x;

[2] Rahmati M B , Ahmadi M , Malekmohamadi, et al. The significance of chest ultrasound and chest X-ray in the diagnosis of children clinically suspected of pneumonia. Journal of Medicine & Life, 2015, 8(Spec Iss 3):50-53.

[3] Joob B , Wiwanitkit V . Chest X-ray and CT findings in H7N9 influenza. Acta Radiologica, 2015, 56(1):NP5-NP5.https://doi.org/10.1177/0284185114549226

[4] Gentile Á, Bakir J, Bialorus L. Impact of the 13-valent pneumococcal conjugate vaccine on the incidence of consolidated pneumonia in children younger than 5 years old in Pilar, Buenos Aires: A population-based study. Archivos Argentinos De Pediatria, 2015, 113(6):502.https://doi.org/10.5546/aap.2015.eng.502

[5] Lin Z Q , Xu X Q , Zhang K B , et al. Chest X-ray and CT findings of early H7N9 avian influenza cases. Acta Radiologica, 2015, 56(5):552-6.. https://doi.org/10.1177/0284185114535209

[6] Liao Caihong, Li Qingxue, Hu Xianhua. Comparison of multi-slice spiral CT three-dimensional imaging and X-ray in evaluating the classification of femoral neck fracture in the elderly patients. Journal of Traumatic Surgery, 2019, 021(006):473-474.

[7] Lin Xizhou. Multi-slice Spiral CT in Diagnosis of Lung Cancer. Chinese and Foreign Medicine,

2018, 037(021):182-183,186.
[8] Chen Hongxia, Duan Minjun, Feng Hongbin. Application value of multislice spiral CT and three-dimensional reconstruction in the diagnosis of scapula fracture. Frontiers of Medicine, 2019, 009(001):52-53.
[9] Lee S M , Cho Y K , Sung Y M , et al. A Case of Pneumonia Caused by Pneumocystis jirovecii Resistant to Trimethoprim-Sulfamethoxazole. Korean Journal of Parasitology, 2015, 53(3):321-327.https://doi.org/10.3347/kjp.2015.53.3.321
[10] Macdonald C , Jayathissa S , Leadbetter M . Is post‐pneumonia chest X‐ray for lung malignancy useful? Results of an audit of current practice. Internal Medicine Journal, 2015, 45(3):329-334.https://doi.org/10.1111/imj.12699
[11] Rahman T , Chowdhury M E H , Khandakar A , et al. Transfer Learning with Deep Convolutional Neural Network (CNN) for Pneumonia Detection using Chest X-ray. Applied ences, 2020, 10(9):3233.https://doi.org/10.3390/app10093233
[12] Ruslie R H , Tjipta D G , Samosir C T , et al. Bacterial pattern and role of laboratory parameters as marker for neonatal sepsis. IOP Conference Series Earth and Environmental ence, 2017, 125(1):012057.https://doi.org/10.1088/1755-1315/125/1/012057
[13] Mittal A , Kumar D , Mittal M , et al. Detecting Pneumonia Using Convolutions and Dynamic Capsule Routing for Chest X-ray Images. Sensors, 2020, 20(Feb):1067-1097.https://doi.org/10.3390/s20041068
[14] Anuradha S , Ghosh S , Dewan R , et al. Fever of Unknown Origin (FUO) in HIV Infection in the Era of Antiretroviral Treatment (ART) in India: Development of a Simple Diagnostic Algorithm.. British Journal of Medicine & Medical Research, 2015, 7(10):839-846.https://doi.org/10.9734/BJMMR/2015/16868
[15] Murad F I , Zanetti Gláucia, Menna B M , et al. Organizing pneumonia: chest HRCT findings. Jornal Brasileiro De Pneumologia, 2015, 41(3):231-237.https://doi.org/10.1590/S1806-37132015000004544
[16] Jimborean G , Ianoi E S , Comes A D , et al. Neuroendocrine pancreatic tumor – Diagnosis circumstances, staging and treatment: A case report. Revue Roumaine De Morphologie Et Embryologie, 2015, 56(2):619.
[17] Ticinesi A , Lauretani F , Nouvenne A , et al. Lung ultrasound and chest x-ray for detecting pneumonia in an acute geriatric ward. Medicine, 2016, 95(27):e4153.https://doi.org/10.1097/MD.0000000000004153
[18] Sui Y , Li J , Zou Z , et al. Comparison of diagnostic value of multislice spiral CT and MRI for different pathological stages of prostate cancer. Oncology Letters, 2019, 17(6):5505-5510.https://doi.org/10.3892/ol.2019.10272
[19] Nair N S , Lewis L E , Lakiang T , et al. Risk factors and barriers to case management of neonatal pneumonia: protocol for a pan-India qualitative study of stakeholder perceptions. Bmj Open, 2017, 7(9):e017403.https://doi.org/10.1136/bmjopen-2017-017403
[20] Sun Huaying, Zhou Liping. Study of Salbutamol and Budesonide for Treatment of Neonatal Pneumonia. Modern Diagnosis and Treatment, 2016, 027(004):648-650.
[21] Lu H , Rui H , Pengxin Y , et al. A correlation study ofCT and clinical features of different clinical types of 2019 novel coronavirus pneumonia. Chinese Journal of Radiology, 2020, 54(00):E003-E003.
[22] Banerjee T , Bhattacharjee A , Upadhyay S , et al. Long-term outbreak of Klebsiella pneumoniae& third generation cephalosporin use in a neonatal intensive care unit in north India. The Indian Journal of Medical Research, 2016, 144(4):622-629.
[23] Basu M . Clinical features and drug sensitivity pattern of Klebsiella pneumoniae sepsis: A descriptive study in a level 2 neonatal care unit in India. Sri Lanka Journal of Child Health, 2017,

46(3):259.https://doi.org/10.4038/sljch.v46i3.8328
[24] Cardenat M , Horo K , Amon-Tanoh-Dick F , et al. Late neonatal pneumonia: The experience of the university hospital of Yopougon in Abidjan. Journal de Pédiatrie et de Puériculture, 2015, 28(1):23-28.https://doi.org/10.1016/j.jpp.2014.10.006
[25] Ahmed Sakr Sherbini Mouhamed. Reducing ventilator-associated pneumonia in neonatal intensive care unit using "VAP prevention Bundle": a cohort study. Bmc Infectious Diseases, 2015, 15(1):314.https://doi.org/10.1186/s12879-015-1062-1